

Deconfinement Dynamics of Fractons in Tilted Bose-Hubbard Chains

Julian Boesl^{1,2}, Philip Zechmann^{1,2}, Johannes Feldmeier³, and Michael Knap^{1,2}

¹Technical University of Munich, TUM School of Natural Sciences, Physics Department, 85748 Garching, Germany

²Munich Center for Quantum Science and Technology (MCQST), Schellingstrasse 4, 80799 München, Germany

³Department of Physics, Harvard University, Cambridge, Massachusetts 02138, USA



(Received 16 November 2023; accepted 15 March 2024; published 2 April 2024)

Fractonic constraints can lead to exotic properties of quantum many-body systems. Here, we investigate the dynamics of fracton excitations on top of the ground states of a one-dimensional, dipole-conserving Bose-Hubbard model. We show that nearby fractons undergo a collective motion mediated by exchanging virtual dipole excitations, which provides a powerful dynamical tool to characterize the underlying ground-state phases. We find that, in the gapped Mott insulating phase, fractons are confined to each other as motion requires the exchange of massive dipoles. When crossing the phase transition into a gapless Luttinger liquid of dipoles, fractons deconfine. Their transient deconfinement dynamics scales diffusively and exhibits strong but subleading contributions described by a quantum Lifshitz model. We examine prospects for the experimental realization in tilted Bose-Hubbard chains by numerically simulating the adiabatic state preparation and subsequent time evolution and find clear signatures of the low-energy fracton dynamics.

DOI: 10.1103/PhysRevLett.132.143401

Introduction.—Fractonic systems, in which elementary excitations exhibit restricted mobility, have attracted much interest over recent years [1–8]. A prominent example are systems that conserve higher multipole moments of a global U(1) charge [9–12]. Such multipole conservation laws drastically impact nonequilibrium properties, entailing Hilbert space fragmentation [13–15], anomalous diffusion [16–20], and a slowdown in the spread of information [21]. A promising approach to realize such phenomena in experimental setups is the preparation of ultracold atomic gases in tilted optical lattices, whose effective behavior is governed by dipole-conserving Bose- or Fermi-Hubbard models. Experimental realizations of such systems have demonstrated subdiffusive dynamics [22] as well as Hilbert space fragmentation [23,24] for high-energy initial states. At low energies, a duality between fractons and elasticity theory indicates a wealth of possible ground-state phases [25–31]. Recent theoretical work has explored such low-energy properties in microscopic dipole-conserving lattice models, establishing Mott insulating phases, Luttinger liquids of dipoles, and supersolids [32–35]. However, preparing and probing such low-energy states in experimental setups remains a significant challenge.

In this work, we examine dynamical probes of fractonic properties using few-fracton excitations on top of the ground states of a dipole-conserving Bose-Hubbard model. We investigate the collective motion of two initially nearby fractons, mediated by virtual dipole excitations, and study how their mobility depends on the underlying ground-state phase (see also the setup discussed in Ref. [36]); see Fig. 1. For the dipole Mott insulator with gapped dipole

excitations, fractons remain confined. By contrast, for the gapless dipole Luttinger liquid, kinematic constraints are eased and we analyze the resulting deconfining dynamics both numerically and analytically. Furthermore, a numerical simulation of adiabatic state preparation demonstrates how the confinement-deconfinement dynamics may be realized with quantum simulators of ultracold atoms in optical lattices. We argue that local dynamical probes are crucial to confirm low-energy dipole-conserving dynamics in lieu of static measurements.

Dipole-conserving Bose-Hubbard model.—We consider a one-dimensional model of lattice bosons with a constrained hopping term [32–34] of the form

$$\hat{H} = -t_d \sum_j (\hat{b}_j^\dagger \hat{b}_{j+1}^2 \hat{b}_{j+2}^\dagger + \text{H.c.}) + \frac{U}{2} \sum_j \hat{n}_j (\hat{n}_j - 1), \quad (1)$$

where t_d is the strength of the correlated hopping and U a repulsive on-site interaction. This Hamiltonian conserves both the total charge (or particle number) $\hat{N} = \sum_j \hat{n}_j$ and the associated dipole moment (or center of mass) $\hat{P} = \sum_j j \hat{n}_j$. Because of the dipole constraint, single charge excitations created by \hat{b}_j^\dagger act as mobility-restricted fractons and can move only by emitting or absorbing a mobile dipole excitation $\hat{d}_j^\dagger \equiv \hat{b}_j^\dagger \hat{b}_{j+1}$; see Fig. 1(a). For a theoretical description of Eq. (1) at low energies, it is convenient to introduce a local dipole charge $\hat{q}_{d,j}$, defined via $\hat{q}_{d,j} = \sum_{\ell=0}^j (\hat{n}_\ell - n)$ [20,34,37]. Here, n is the average charge density, and we take $n \in \mathbb{N}$ to be integer throughout

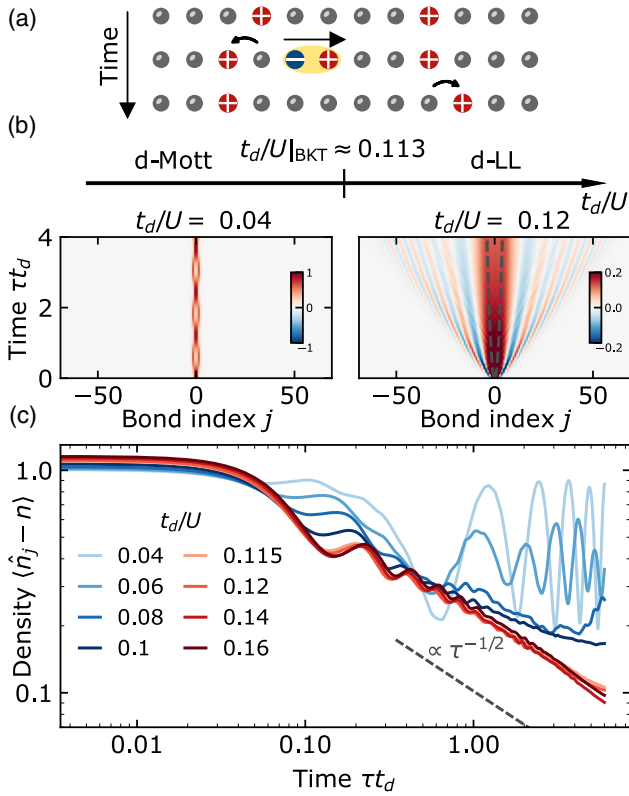


FIG. 1. Deconfinement of two fractons. (a) Fractons in dipole-moment-conserving systems move collaboratively by exchanging dipoles [36]. (b) Time evolution of the excess density $\langle \hat{n}_j(\tau) - n \rangle$ after adding two particles at adjacent sites on top of the ground state at filling $n = 2$. Deep in the dipole Mott insulator (left), the confined particles follow a breathing motion. In the dipole Luttinger liquid (right), they spread diffusively over accessible timescales in accordance with a semiclassical picture (dashed gray line). (c) Time evolution of the local excess density $\langle \hat{n}_0(\tau) - n \rangle$ on a site where a particle was added. The excess density remains finite for the Mott state but decays diffusively in the Luttinger liquid.

this work. Crucially, assuming a finite energy gap for single charge excitations, the local dipole charge $q_{d,j}$ remains bounded in the ground state of Eq. (1) [34]. A standard bosonization procedure gives a counting field $\phi(x)$ and phase field $\theta(x)$ for the fractons, which satisfy $[\partial_x \phi(x), \theta(x')] = -i\pi\delta(x - x')$ [38]. Considering the definition of the dipole density $\hat{q}_{d,j}$, one can bosonize the dipole degrees of freedom to find the relation between the fracton and the dipole fields $\partial_x \phi_d(x) = \phi(x)$ and $\theta_d(x) = -\partial_x \theta(x)$ leading to equivalent commutation relations $[\partial_x \phi_d(x), \theta_d(x')] = -i\pi\delta(x - x')$ (for details, see Supplemental Material [39]). The effective low-energy description of the system is then given by the sine-Gordon model [33,34]

$$H_{\text{SG}} = \int \frac{dx}{2\pi} \left\{ u_d K_d (\partial_x \theta_d)^2 + \frac{u_d}{K_d} (\partial_x \phi_d)^2 + g \cos(\phi_d) \right\}, \quad (2)$$

with Luttinger parameter K_d and Luttinger velocity u_d . For $K_d < 2$, realized at small hopping t_d/U , the cosine is relevant, pinning the counting field $\phi_d(x)$ and driving the system into a Mott insulator of dipoles with finite mass gap. At a critical hopping strength $t_d/U|_{\text{BKT}} \approx 0.113$, the system undergoes a Berezinskii-Kosterlitz-Thouless (BKT) transition at $K_d = 2$ as the cosine becomes irrelevant. The dipole gap closes and the system enters a Luttinger liquid of dipoles:

$$H_{\text{LL}} = \frac{u_d}{2\pi} \int dx \left\{ K_d (\partial_x \theta_d)^2 + \frac{1}{K_d} (\partial_x \phi_d)^2 \right\}. \quad (3)$$

Previous numerical studies demonstrated that the lowest integer filling at which a transition into this Luttinger liquid occurs is $n = 2$, with $t_d/U|_{\text{BKT}} \approx 0.113$ [34]. We, thus, restrict to $n = 2$ for the remainder of this work, operating within the phase diagram shown in Fig. 1(b).

Two-fracton dynamics.—We consider the ground states $|\Omega\rangle$ of the dipole-conserving Bose-Hubbard model Eq. (1) and add two particles on adjacent sites $|\psi_{2F}\rangle = \hat{b}_0^\dagger \hat{b}_1^\dagger |\Omega\rangle$. We note that $|\Omega\rangle = |\Omega(t_d/U)\rangle$ depends on the ratio t_d/U . Time evolving $|\psi_{2F}\rangle$ under \hat{H} , the fractons can hop in opposite directions by the exchange of virtual dipoles acting as “force carriers,” reminiscent of mediated interactions in gauge theories [35,36,52]; see Fig. 1(a). Our goal is to determine the dependence of this dynamical process on the underlying ground state.

We first discuss the Mott insulating phase. Deep in the strong-coupling limit $t_d/U \ll 1$, the ground state $|\Omega\rangle \approx |222\dots\rangle$ is close to the homogeneously filled state. The dynamics then takes place in a degenerate subspace spanned by the states $|r\rangle \equiv \hat{b}_{-r}^\dagger \hat{b}_{1+r}^\dagger |\Omega\rangle$, in which the left (right) particle excitation is shifted r sites to the left (right) from its original position. The initial state is given by $|\psi_{2F}\rangle = |r=0\rangle$. The degeneracy of this subspace is subsequently lifted by exchanging a single virtual dipole carrying an energy cost $\propto U$. In degenerate perturbation theory, we obtain an effective Hamiltonian

$$\hat{H}_{2F} = - \sum_{r \geq 0} J_r |r+1\rangle \langle r| + \text{H.c.}, \quad (4)$$

with a position-dependent hopping $J_r \propto t_d^2/U \exp(-r/\xi)$ that decays exponentially over a distance ξ determined by the ratio t_d/U (for details, see Supplemental Material [39]). The exponential suppression arises as the massive dipole has to travel further to transmit the interaction, dynamically *confining* the two fractons [36]. At very strong repulsion $t_d/U \ll 1$, only the states $|r=0\rangle$ and $|r=1\rangle$ contribute significantly to the dynamics, leading to a periodic breathing motion between these states. To substantiate this picture of confinement on top of the Mott insulator, even away from $t_d/U \ll 1$, we perform matrix product state (MPS) simulations for the model Eq. (1). We compute the microscopic ground state $|\Omega\rangle$, add two particles on sites 0 and 1,

and evaluate the time-evolved local excess densities $\langle \hat{n}_j(\tau) - n \rangle \equiv \langle \psi_{2F} | e^{i\hat{H}\tau} \hat{n}_j e^{-i\hat{H}\tau} | \psi_{2F} \rangle - n$. Throughout the Mott insulator, the excess density $\langle \hat{n}_0(\tau) - n \rangle$ at the initial position of a fracton excitation retains a finite long-time value, in agreement with confinement; see Fig. 1(c), blue curves. At very small t_d/U , oscillations in $\langle \hat{n}_0(\tau) - n \rangle$ become apparent. The full spatiotemporal profile of $\langle \hat{n}_j(\tau) - n \rangle$ shown in Fig. 1(b), left panel, reveals that this is indeed due to the breathing motion of the confined fractons.

Moving across the phase transition into the dipole Luttinger liquid, the gap of the dipole exchange particles closes, lifting the exponential suppression of the correlated hopping. We thus expect the two fractons to *deconfine* and propagate apart. In a semiclassical picture, we assume that the rate $dr/d\tau$ at which the distance r between the fractons increases is determined by the time r/u_d it takes a dipole at velocity u_d to travel between them, i.e., $(dr/d\tau) \propto r^{-1}$. This leads to a diffusive space-time scaling $r \propto \sqrt{\tau}$. We observe dynamics consistent with this semiclassical description on numerically accessible timescales in the diffusive decay of $\langle \hat{n}_0(\tau) - n \rangle \sim 1/\sqrt{\tau}$ throughout the Luttinger liquid; see Fig. 1(c), red curves. This diffusive transport is reflected in the full profile of the excess density $\langle \hat{n}_j(\tau) - n \rangle$, which in the center of the system broadens as $\sqrt{\tau}$; see Fig. 1(b), right panel. However, intriguingly, $\langle \hat{n}_j(\tau) - n \rangle$ further exhibits strong oscillations beyond this feature, spreading behind a ballistically moving light cone and bending in a seemingly diffusive fashion. In order to explain the origin of this feature, we will examine the dynamics of local dipole excitations in the following.

Local dipole excitation.—In addition to fracton excitations, we can directly study the “force-carrying” dipole excitations by considering the initial state $|\psi_D\rangle = \hat{b}_0^\dagger \hat{b}_1 |\Omega\rangle$. Deep in the Mott insulator, the effective Hamiltonian governing the dynamics of the dipole excitation corresponds to a single particle nearest-neighbor hopping model (see Ref. [39] for details). The dipole excitation, thus, spreads ballistically. We confirm this numerically by evaluating the time-evolved local dipole charges $\langle \hat{q}_{d,j}(\tau) \rangle \equiv \langle \psi_D | e^{i\hat{H}\tau} \hat{q}_{d,j} e^{-i\hat{H}\tau} | \psi_D \rangle$; see Fig. 2(a).

Turning to the dipole Luttinger liquid, the low-energy model Eq. (3) predicts two sharp sound modes in the dipole charge $\langle \hat{q}_{d,j}(\tau) \rangle$, moving right or left with velocity $\pm u_d$ and yielding a dynamical exponent $z = 1$. Our numerical results indeed indicate the emergence of these sound modes at the latest accessible times; see Fig. 2(b). The observed dipole density is not inversion symmetric around the origin of the excitation, since the Hamiltonian is not particle-hole symmetric. However, similar to the two-fracton case discussed before, the finite-time dynamics is characterized by additional, strongly oscillating contributions. This suggests the following picture: While Eq. (3) provides the correct *asymptotic* description for late times and low energies,

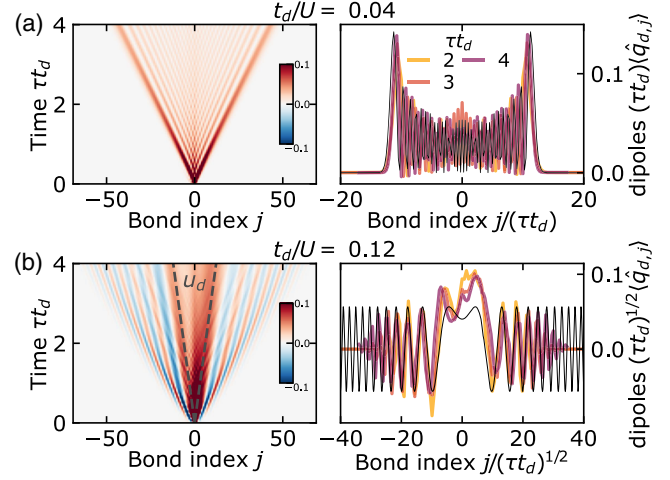


FIG. 2. Dynamics of a dipole. Time evolution of an additional dipole on top of the $n = 2$ ground state. Left column: dipole charge $\langle \hat{q}_{d,j}(\tau) \rangle$. Right column: rescaled dipole density cuts at several times. (a) A dipole excitation on top of the Mott insulator expands ballistically and is effectively described by a single free particle (black line, evaluated at $t_d\tau = 4$). (b) A dipole excitation in the Luttinger liquid exhibits pronounced diffusive waves at early times, obeying the Lifshitz scaling relation Eq. (6) (black line). The late-time dynamics are eventually dominated by the ballistic Luttinger modes (dashed lines).

subleading corrections to Eq. (3) are important on accessible, finite times.

In order to understand these corrections, we recall that Eq. (3) provides the correct low-energy description of the microscopic Hamiltonian Eq. (1) in the presence of a finite gap for single charge excitations. Previous studies have established a finite charge gap for all t_d/U [33,34]. However, in practice, this gap can become very small, and at finite times the system appears as if charge excitations were gapless. According to the fracton-dipole field relations, the finite charge gap is due to the second term $\sim [\partial_x \phi_d(x)]^2 = \phi^2(x)$ in Eq. (3). Assuming this term is small, we drop it for the purpose of effectively describing early-time dynamics. Including the next-to-leading-order term $\sim [\partial_x^2 \phi_d(x)]^2$ then gives rise to a quantum Lifshitz model [32,53,54]:

$$H_{\text{Lif}} = \frac{v}{2\pi} \int dx \left(K(\partial_x \theta_d)^2 + \frac{1}{K}(\partial_x^2 \phi_d)^2 \right), \quad (5)$$

which we express in dipole degrees of freedom and where the parameters v and K are named in analogy to the Hamiltonian (3). The energy spectrum follows a quadratic relation $\omega \propto k^2$ and induces a dynamical exponent $z = 2$. A recent numerical study of the dipole spectral function in the Luttinger liquid indeed confirmed a quadratic dispersion at higher energies [55]. We discuss the relation between the two field theories Eqs. (3) and (5) in detail in Supplemental Material [39]. Using Eq. (5) as an

approximation for early times, we evaluate the time-evolved dipole charge in closed form:

$$\langle \hat{q}_{d,j}(\tau) \rangle \propto \begin{cases} \delta(j), & \tau = 0 \\ \frac{1}{2\sqrt{v\tau}} \left[\cos\left(\frac{j^2}{4v\tau}\right) + \sin\left(\frac{j^2}{4v\tau}\right) \right], & \text{else.} \end{cases} \quad (6)$$

This oscillating function follows a diffusive scaling as expected from the dynamical exponent $z = 2$.

This expression violates Lieb-Robinson bounds on information spreading; however, causal behavior is restored by a high-momentum cutoff $\Lambda = \mathcal{O}(1/a)$, which in a lattice system is naturally set by the lattice spacing a . The cutoff induces a light cone with finite velocity that approximately corresponds to the group velocity of the quadratic Lifshitz dispersion at the momentum cutoff, $\partial_k \omega(k)|_{\Lambda} = 2v\Lambda$.

Our numerical results for the early-time dipole dynamics agree remarkably well with the scaling relation predicted by the Lifshitz theory; see Fig. 2(b), right column. Also indicated is the Luttinger velocity, extracted from ground-state numerics of the Luttinger parameter K_d and the dipole compressibility κ_d using the relation $\kappa_d = K_d/u_d\pi$ [34], which is slow compared to the diffusive Lifshitz oscillations. These oscillations are inherited in the two-fracton case discussed previously and constitute a process distinct from the virtual dipole exchange between fractons.

Experimental realization: Tilted lattices.—Having established the dynamics of few-fracton initial states as characteristic signatures of the underlying dipole Mott insulator and Luttinger liquid phases, we now turn to the question of how to realize these phases and their dynamical signatures in experiments. An accessible platform to implement dipole-conserving dynamics are ultracold gases of atoms in an optical lattice with a strong tilt. The Hamiltonian of such a system is given by

$$\hat{H} = -t \sum_j (\hat{b}_j^\dagger \hat{b}_{j+1} + \text{H.c.}) + \frac{U}{2} \sum_j \hat{n}_j (\hat{n}_j - 1) + \Delta \sum_j j \hat{n}_j, \quad (7)$$

where Δ is the strength of the tilt. In the limit of strong $\Delta \gg t, U$, only correlated processes that conserve the total dipole moment are energetically allowed. A Schrieffer-Wolff transformation yields the dipole-conserving Hamiltonian (1) with effective correlated hopping $t_{d,\text{eff}} = t^2 U / \Delta^2$ and a renormalized $U_{\text{eff}} = U(1 - 4t^2 / \Delta^2)$, alongside a nearest-neighbor interaction of strength $2t^2 U / \Delta^2$ [14,23,24,56]; see Supplemental Material [39] for the full derivation.

The first step is to prepare low-energy states within sectors of fixed dipole moment at integer filling. We propose the following protocol: (i) Initialize the system in a homogeneous state $|222\dots\rangle$ at integer filling at vanishing hopping $t = 0$ and zero tilt $\Delta = 0$. (ii) The tilt

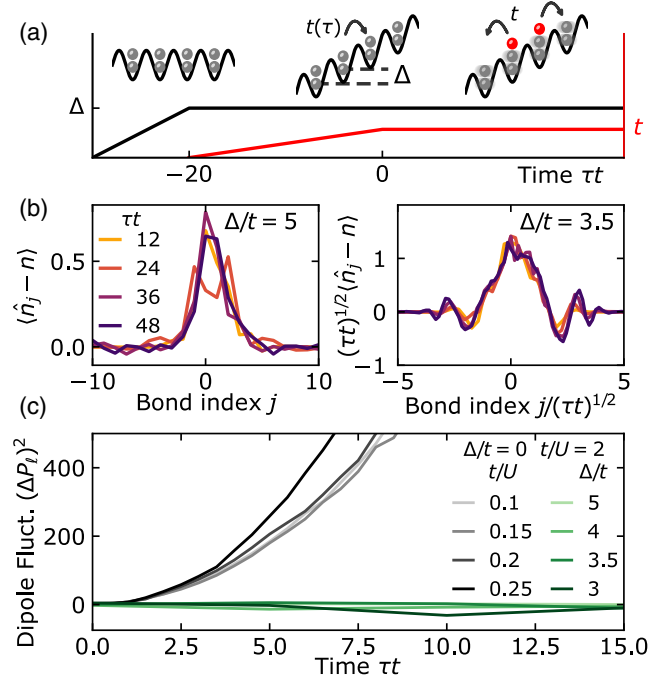


FIG. 3. Fractonic dynamics in a tilted lattice. (a) Sequence for adiabatic preparation of ground states with a two-particle excitation. After a rapid ramp of the tilt Δ , the hopping strength is slowly increased to a finite value t . Subsequently, additional particles are introduced for example by optical tweezer potentials. (b) Density profile of the two-particle state for weak (left) and strong (right) final hopping strength. Weak hopping results in the predicted breathing motion. For strong hopping, Lifshitz-like oscillations emerge, with an approximately diffusive scaling. Inversion symmetry is explicitly broken due to the linear potential. (c) Time evolution of dipole moment fluctuations in a segment of size $\ell = 80$ after preparing the excitations on top of an $n = 2$ state. The dipole fluctuations in the tilted lattice do not increase over a significant period of time, suggesting dipole-conserving dynamics (green lines). By contrast, fluctuations on top of a conventional (untitled) $n = 1$ Mott state increase quadratically (gray lines). Fluctuations of adiabatically prepared ground states are subtracted in both cases.

is then ramped up quickly to a value Δ , leaving the state invariant. This realizes the ground state of the dipole Mott insulator in the limit of vanishing correlated hopping, $t_{d,\text{eff}} = 0$. (iii) Next, the depth of the optical lattice is lowered adiabatically, increasing t (and, thus, $t_{d,\text{eff}}$) until the desired point in the phase diagram is reached; see Fig. 3(a). This results in a state $|\tilde{\Omega}\rangle$ that depends on the final values t , Δ , and U of hopping, tilt, and interactions, as well as the specific adiabatic ramp. (iv) Finally, additional particles on top of $|\tilde{\Omega}\rangle$ may be introduced to create the state $|\tilde{\psi}_{2F}\rangle = \hat{b}_0^\dagger \hat{b}_1^\dagger |\tilde{\Omega}\rangle$, for example, using optical tweezers; see, e.g., Refs. [57–59]. Other excitations may be probed as well: Using digital micromirror devices, tunneling between neighboring sites can be induced to access a single-dipole state $|\tilde{\psi}_D\rangle = \hat{b}_0^\dagger \hat{b}_1 |\tilde{\Omega}\rangle$. One can also dope holes in a similar

vein; as we can expect hole dynamics over a sufficiently high-filling background to resemble that of particle excitations, this strategy can likewise be used to study single- and few-fracton states.

To demonstrate this protocol, we numerically simulate the adiabatic preparation of $|\tilde{\Omega}\rangle$ and the subsequent dynamics from the two-particle excitation state $|\tilde{\psi}_{2F}\rangle$ using MPS methods. For a given final value t of the single particle hopping, we set $U = 0.5t$ and allocate a time $\tau t = 20$ for a linear adiabatic ramp; see Fig. 3(a). We show the dynamics of the excess charge $\langle \hat{n}_j(\tau) - n \rangle$ from the two-particle state $|\tilde{\psi}_{2F}\rangle$ in Fig. 3(b). For weak hopping, $\Delta/t = 5$, the fractons remain confined with clear signatures of breathing dynamics, distinct from the much faster Bloch oscillations induced by the linear potential. In contrast, for larger final hopping, $\Delta/t = 3.5$, we observe dynamical deconfinement of the fractons. The spread of the excess density $\langle \hat{n}_j(\tau) - n \rangle$ scales approximately diffusively, with strong oscillations reminiscent of the scaling function (6). This suggests that the dynamical properties of the dipole Luttinger liquid—including strong subleading contributions from a quantum Lifshitz model—are well captured in this setup.

It remains to verify that the observed diffusive charge dynamics is indeed dipole conserving. For this purpose, we define the dipole moment $\hat{P}_\ell = \sum_{j=1}^\ell \hat{q}_{d,j-\ell/2}$ in a large linear segment of size ℓ around position $j = 0$. In experiment, \hat{P}_ℓ can be measured from snapshots using quantum gas microscopes [60,61]. We then consider *fluctuations* of the time-evolved dipole moment $\hat{P}_\ell(\tau)$, which we label as $(\Delta P_\ell^{(2F)}(\tau))^2$ for the initial state $|\tilde{\psi}_{2F}\rangle$ and $(\Delta P_\ell^{(\Omega)}(\tau))^2$ for $|\tilde{\Omega}\rangle$. We note that the latter are nontrivial, since $|\tilde{\Omega}\rangle$ is not a true eigenstate. The difference $(\Delta P_\ell(\tau))^2 \equiv (\Delta P_\ell^{(2F)}(\tau))^2 - (\Delta P_\ell^{(\Omega)}(\tau))^2$ then quantifies the fluctuation of the dipole moment due to dynamics of charge excitations. We numerically evaluate the dynamics of $(\Delta P_\ell(\tau))^2$ for a segment of $\ell = 80$ and for different tilt-to-hopping ratios Δ/t ; see Fig. 3(c) (green lines). The fluctuations do not increase, confirming effective dipole conservation on a prethermal timescale. By contrast, the dipole fluctuations from two charge excitations on top of a regular $n = 1$ Mott insulator with vanishing tilt $\Delta = 0$ increase rapidly (gray lines). In this case, we predict that the free ballistic movement of the particles leads to $(\Delta P_\ell(\tau))^2 \sim \tau^2$ at late times, consistent with our numerical results.

Finally, one may be tempted to probe the static fluctuations $(\Delta P_\ell^{(\Omega)})^2$ of the state $|\tilde{\Omega}\rangle$ directly: For the ground states of the model Eq. (1) with exact dipole conservation, these fluctuations scale with ℓ as $(\Delta P_\ell^{(\text{dMI})})^2 \sim \text{const}$ in the dipole Mott insulator and $(\Delta P_\ell^{(\text{dLL})})^2 \sim \log(\ell)$ in the dipole Luttinger liquid (analogous to particle number fluctuations in a regular Mott state or Luttinger liquid [62–64]). By contrast, in a regular Mott insulator without dipole

conservation, a finite density of particle-hole fluctuations leads to $(\Delta P_\ell^{(\text{MI})})^2 \sim \ell$, providing a clear distinction to dipole-conserving states. Crucially, however, the tilted model Eq. (7) enforces dipole conservation in a rotated basis given by a Schrieffer-Wolff transformation. Since measurements are taken in the standard occupation number basis, this mismatch leads to $(\Delta P_\ell^{(\Omega)})^2 \sim \ell$ despite effective dipole conservation because of the “wrong” measurement basis.

Conclusions and outlook.—We have studied the dynamics of local excitations on top of the integer-filling ground states of the dipolar Bose-Hubbard model. Fractons undergo a confinement-deconfinement transition when tuning the initial state from a dipole Mott insulator to a dipole Luttinger liquid. Future work may be dedicated to developing an effective theory of the collective fracton motion and to elucidating its eventual asymptotic late-time behavior. Moreover, it would be interesting to explore the consequences of a modified Mermin-Wagner theorem for our protocols in higher-dimensional dipole-moment-conserving systems [32,65,66].

We have furthermore studied the adiabatic preparation and subsequent dynamics of the two-fracton state in a tilted optical lattice setup, identifying dynamical probes as crucial tools to observe fractonic properties at low energies. Our results present clear strategies to realize and probe fractonic low-energy phases. Future studies may explore noninteger commensurate fillings which realize metastable supersolids [33,34]. Quasi-two-dimensional gases of polar molecules may offer alternative routes to study fracton deconfinement dynamics, as those systems are effectively described by the elasticity theory of two-dimensional quantum crystals, and, in fact, supersolid phases have already been demonstrated experimentally [67].

Numerical data and simulation codes are available on Zenodo upon reasonable request [68].

We thank Brice Bakkali-Hassani, Immanuel Bloch, Sooshin Kim, and Johannes Zeiher for insightful discussions. We acknowledge support from the Deutsche Forschungsgemeinschaft (DFG, German Research Foundation) under Germany’s Excellence Strategy—EXC–2111–390814868 and DFG Grants No. KN1254/1-2, No. KN1254/2-1, and No. TRR 360-492547816, and the European Research Council (ERC) under the European Union’s Horizon 2020 research and innovation program (Grant Agreement No. 851161), as well as the Munich Quantum Valley, which is supported by the Bavarian state government with funds from the Hightech Agenda Bayern Plus. J. F. acknowledges support by the Harvard Quantum Initiative. Matrix product state simulations were performed using the TENPY package [69].

- [1] R. M. Nandkishore and M. Hermele, Fractons, *Annu. Rev. Condens. Matter Phys.* **10**, 295 (2019).
- [2] M. Pretko, X. Chen, and Y. You, Fracton phases of matter, *Int. J. Mod. Phys. A* **35**, 2030003 (2020).
- [3] A. Gromov and L. Radzihovsky, Colloquium: Fracton matter, *Rev. Mod. Phys.* **96**, 011001 (2024).
- [4] C. Chamon, Quantum glassiness in strongly correlated clean systems: An example of topological overprotection, *Phys. Rev. Lett.* **94**, 040402 (2005).
- [5] J. Haah, Local stabilizer codes in three dimensions without string logical operators, *Phys. Rev. A* **83**, 042330 (2011).
- [6] S. Bravyi and J. Haah, Quantum self-correction in the 3d cubic code model, *Phys. Rev. Lett.* **111**, 200501 (2013).
- [7] B. Yoshida, Exotic topological order in fractal spin liquids, *Phys. Rev. B* **88**, 125122 (2013).
- [8] S. Vijay, J. Haah, and L. Fu, A new kind of topological quantum order: A dimensional hierarchy of quasiparticles built from stationary excitations, *Phys. Rev. B* **92**, 235136 (2015).
- [9] M. Pretko, Subdimensional particle structure of higher rank $u(1)$ spin liquids, *Phys. Rev. B* **95**, 115139 (2017).
- [10] M. Pretko, Generalized electromagnetism of subdimensional particles: A spin liquid story, *Phys. Rev. B* **96**, 035119 (2017).
- [11] M. Pretko, Higher-spin Witten effect and two-dimensional fracton phases, *Phys. Rev. B* **96**, 125151 (2017).
- [12] M. Pretko, The fracton gauge principle, *Phys. Rev. B* **98**, 115134 (2018).
- [13] P. Sala, T. Rakovszky, R. Verresen, M. Knap, and F. Pollmann, Ergodicity breaking arising from Hilbert space fragmentation in dipole-conserving Hamiltonians, *Phys. Rev. X* **10**, 011047 (2020).
- [14] V. Khemani, M. Hermele, and R. Nandkishore, Localization from Hilbert space shattering: From theory to physical realizations, *Phys. Rev. B* **101**, 174204 (2020).
- [15] T. Rakovszky, P. Sala, R. Verresen, M. Knap, and F. Pollmann, Statistical localization: From strong fragmentation to strong edge modes, *Phys. Rev. B* **101**, 125126 (2020).
- [16] A. Gromov, A. Lucas, and R. M. Nandkishore, Fracton hydrodynamics, *Phys. Rev. Res.* **2**, 033124 (2020).
- [17] J. Feldmeier, P. Sala, G. De Tomasi, F. Pollmann, and M. Knap, Anomalous diffusion in dipole- and higher-moment-conserving systems, *Phys. Rev. Lett.* **125**, 245303 (2020).
- [18] A. Morningstar, V. Khemani, and D. A. Huse, Kinetically constrained freezing transition in a dipole-conserving system, *Phys. Rev. B* **101**, 214205 (2020).
- [19] P. Zhang, Subdiffusion in strongly tilted lattice systems, *Phys. Rev. Res.* **2**, 033129 (2020).
- [20] S. Moudgalya, A. Prem, D. A. Huse, and A. Chan, Spectral statistics in constrained many-body quantum chaotic systems, *Phys. Rev. Res.* **3**, 023176 (2021).
- [21] J. Feldmeier and M. Knap, Critically slow operator dynamics in constrained many-body systems, *Phys. Rev. Lett.* **127**, 235301 (2021).
- [22] E. Guardado-Sanchez, A. Morningstar, B. M. Spar, P. T. Brown, D. A. Huse, and W. S. Bakr, Subdiffusion and heat transport in a tilted two-dimensional Fermi-Hubbard system, *Phys. Rev. X* **10**, 011042 (2020).
- [23] S. Scherg, T. Kohlert, P. Sala, F. Pollmann, B. Hebbe Madhusudhana, I. Bloch, and M. Aidelsburger, Observing non-ergodicity due to kinetic constraints in tilted Fermi-Hubbard chains, *Nat. Commun.* **12**, 4490 (2021).
- [24] T. Kohlert, S. Scherg, P. Sala, F. Pollmann, B. Hebbe Madhusudhana, I. Bloch, and M. Aidelsburger, Exploring the regime of fragmentation in strongly tilted Fermi-Hubbard chains, *Phys. Rev. Lett.* **130**, 010201 (2023).
- [25] M. Pretko and L. Radzihovsky, Fracton-elasticity duality, *Phys. Rev. Lett.* **120**, 195301 (2018).
- [26] A. Gromov, Chiral topological elasticity and fracton order, *Phys. Rev. Lett.* **122**, 076403 (2019).
- [27] M. Pretko, Z. Zhai, and L. Radzihovsky, Crystal-to-fracton tensor gauge theory dualities, *Phys. Rev. B* **100**, 134113 (2019).
- [28] A. Kumar and A. C. Potter, Symmetry-enforced fractonicity and two-dimensional quantum crystal melting, *Phys. Rev. B* **100**, 045119 (2019).
- [29] Z. Zhai and L. Radzihovsky, Two-dimensional melting via Sine-Gordon duality, *Phys. Rev. B* **100**, 094105 (2019).
- [30] L. Radzihovsky, Quantum smectic gauge theory, *Phys. Rev. Lett.* **125**, 267601 (2020).
- [31] Z. Zhai and L. Radzihovsky, Fractonic gauge theory of smectics, *Ann. Phys. (Amsterdam)* **435**, 168509 (2021), Special Issue on Philip W. Anderson.
- [32] E. Lake, M. Hermele, and T. Senthil, Dipolar Bose-Hubbard model, *Phys. Rev. B* **106**, 064511 (2022).
- [33] E. Lake, H.-Y. Lee, J. H. Han, and T. Senthil, Dipole condensates in tilted Bose-Hubbard chains, *Phys. Rev. B* **107**, 195132 (2023).
- [34] P. Zechmann, E. Altman, M. Knap, and J. Feldmeier, Fractonic luttinger liquids and supersolids in a constrained Bose-Hubbard model, *Phys. Rev. B* **107**, 195131 (2023).
- [35] E. Lake and T. Senthil, Non-Fermi liquids from kinetic constraints in tilted optical lattices, *Phys. Rev. Lett.* **131**, 043403 (2023).
- [36] M. Pretko, Emergent gravity of fractons: Mach's principle revisited, *Phys. Rev. D* **96**, 024051 (2017).
- [37] X. Feng and B. Skinner, Hilbert space fragmentation produces an effective attraction between fractons, *Phys. Rev. Res.* **4**, 013053 (2022).
- [38] T. Giamarchi, *Quantum Physics in One Dimension* (Oxford University Press, New York, 2003).
- [39] See Supplemental Material at <http://link.aps.org/supplemental/10.1103/PhysRevLett.132.143401>, which also includes the following Refs. [40–51] for technical details and additional information, including on numerics.
- [40] P. Gorantla, H. T. Lam, N. Seiberg, and S.-H. Shao, Global dipole symmetry, compact Lifshitz theory, tensor gauge theory, and fractons, *Phys. Rev. B* **106**, 045112 (2022).
- [41] S. Bravyi, D. P. DiVincenzo, and D. Loss, Schrieffer–Wolff transformation for quantum many-body systems, *Ann. Phys. (Amsterdam)* **326**, 2793 (2011).
- [42] A. Rosch, D. Rasch, B. Binz, and M. Vojta, Metastable superfluidity of repulsive fermionic atoms in optical lattices, *Phys. Rev. Lett.* **101**, 265301 (2008).
- [43] G. H. Wannier, Wave functions and effective Hamiltonian for Bloch electrons in an electric field, *Phys. Rev.* **117**, 432 (1960).

- [44] S. R. White, Density matrix formulation for quantum renormalization groups, *Phys. Rev. Lett.* **69**, 2863 (1992).
- [45] S. R. White, Density-matrix algorithms for quantum renormalization groups, *Phys. Rev. B* **48**, 10345 (1993).
- [46] G. Vidal, Classical simulation of infinite-size quantum lattice systems in one spatial dimension, *Phys. Rev. Lett.* **98**, 070201 (2007).
- [47] S. Singh, R. N. C. Pfeifer, and G. Vidal, Tensor network decompositions in the presence of a global symmetry, *Phys. Rev. A* **82**, 050301(R) (2010).
- [48] S. Singh, R. N. C. Pfeifer, and G. Vidal, Tensor network states and algorithms in the presence of a global U(1) symmetry, *Phys. Rev. B* **83**, 115125 (2011).
- [49] C. Hubig, I. P. McCulloch, U. Schollwöck, and F. A. Wolf, Strictly single-site DMRG algorithm with subspace expansion, *Phys. Rev. B* **91**, 155115 (2015).
- [50] M. P. Zaletel, R. S. K. Mong, C. Karrasch, J. E. Moore, and F. Pollmann, Time-evolving a matrix product state with long-ranged interactions, *Phys. Rev. B* **91**, 165112 (2015).
- [51] G. Vidal, Efficient simulation of one-dimensional quantum many-body systems, *Phys. Rev. Lett.* **93**, 040502 (2004).
- [52] A. Prakash, A. Goriely, and S. L. Sondhi, Classical non-relativistic fractons, *Phys. Rev. B* **109**, 054313 (2024).
- [53] J.-K. Yuan, S. A. Chen, and P. Ye, Fractonic superfluids, *Phys. Rev. Res.* **2**, 023267 (2020).
- [54] L. Radzihovsky, Lifshitz gauge duality, *Phys. Rev. B* **106**, 224510 (2022).
- [55] P. Zechmann, J. Boesl, J. Feldmeier, and M. Knap, Dynamical spectral response of fractonic quantum matter, *Phys. Rev. B* **109**, 125137 (2024).
- [56] S. Moudgalya, A. Prem, R. Nandkishore, N. Regnault, and B. A. Bernevig, Thermalization and its absence within Krylov subspaces of a constrained Hamiltonian, in *Memorial Volume for Shoucheng Zhang* (World Scientific, Singapore, 2022), pp. 147–209.
- [57] A. W. Young, W. J. Eckner, N. Schine, A. M. Childs, and A. M. Kaufman, Tweezer-programmable 2d quantum walks in a Hubbard-regime lattice, *Science* **377**, 885 (2022).
- [58] A. W. Young, S. Geller, W. J. Eckner, N. Schine, S. Glancy, E. Knill, and A. M. Kaufman, An atomic boson sampler, [arXiv:2307.06936](https://arxiv.org/abs/2307.06936).
- [59] R. Tao, M. Ammenwerth, F. Gyger, I. Bloch, and J. Zeiher, High-fidelity detection of large-scale atom arrays in an optical lattice, [arXiv:2309.04717](https://arxiv.org/abs/2309.04717).
- [60] W. S. Bakr, J. I. Gillen, A. Peng, S. Fölling, and M. Greiner, A quantum gas microscope for detecting single atoms in a Hubbard-regime optical lattice, *Nature (London)* **462**, 74 (2009).
- [61] J. F. Sherson, C. Weitenberg, M. Endres, M. Cheneau, I. Bloch, and S. Kuhr, Single-atom-resolved fluorescence imaging of an atomic Mott insulator, *Nature (London)* **467**, 68 (2010).
- [62] H. F. Song, S. Rachel, and K. Le Hur, General relation between entanglement and fluctuations in one dimension, *Phys. Rev. B* **82**, 012405 (2010).
- [63] A. G. Abanov, D. A. Ivanov, and Y. Qian, Quantum fluctuations of one-dimensional free fermions and Fisher–Hartwig formula for Toeplitz determinants, *J. Phys. A* **44**, 485001 (2011).
- [64] S. Rachel, N. Laflorencie, H. F. Song, and K. Le Hur, Detecting quantum critical points using bipartite fluctuations, *Phys. Rev. Lett.* **108**, 116401 (2012).
- [65] C. Stahl, E. Lake, and R. Nandkishore, Spontaneous breaking of multipole symmetries, *Phys. Rev. B* **105**, 155107 (2022).
- [66] C. Stahl, M. Qi, P. Glorioso, A. Lucas, and R. Nandkishore, Fracton superfluid hydrodynamics, *Phys. Rev. B* **108**, 144509 (2023).
- [67] L. Chomaz, D. Petter, P. Ilzhöfer, G. Natale, A. Trautmann, C. Politi, G. Durastante, R. M. W. van Bijnen, A. Patscheider, M. Sohmen, M. J. Mark, and F. Ferlaino, Long-lived and transient supersolid behaviors in dipolar quantum gases, *Phys. Rev. X* **9**, 021012 (2019).
- [68] All data and simulation codes are available upon reasonable request at [10.5281/zenodo.10035551](https://doi.org/10.5281/zenodo.10035551).
- [69] J. Hauschild and F. Pollmann, Efficient numerical simulations with tensor networks: Tensor Network Python (TENPY), *SciPost Phys. Lect. Notes* **5** (2018).